

Wolfgang E. Nagel
Dietmar H. Kröner
Michael M. Resch *Editors*

High Performance Computing in Science and Engineering '15

H L R I S

 Springer

High Performance Computing in Science and Engineering '15

Wolfgang E. Nagel • Dietmar H. Kröner •
Michael M. Resch
Editors

High Performance Computing in Science and Engineering '15

Transactions of the High Performance
Computing Center, Stuttgart (HLRS) 2015

 Springer

Editors

Wolfgang E. Nagel
Zentrum für Informationsdienste
und Hochleistungsrechnen (ZIH)
Technische Universität Dresden
Dresden
Germany

Dietmar H. Kröner
Abteilung für Angewandte Mathematik
Universität Freiburg
Freiburg
Germany

Michael M. Resch
Höchstleistungsrechenzentrum
Stuttgart (HLRS)
Universität Stuttgart
Stuttgart
Germany

Front cover figure: Turbulent wake of a wind turbine rotor predicted by Detached Eddy Simulation. The vortex system is colored by axial velocity. Massive flow separation is present in the hub region where vortices interact with each other at different length scales. Details can be found in “Evaluation and Control of Loads on Wind Turbines under Different Operating Conditions by means of CFD”, by C. Schulz, A. Fischer, P. Weihing, T. Lutz, and E. Krämer, Institute of Aerodynamics and Gas Dynamics, University of Stuttgart, Stuttgart, Germany, on page 463ff.

ISBN 978-3-319-24631-4 ISBN 978-3-319-24633-8 (eBook)
DOI 10.1007/978-3-319-24633-8

Library of Congress Control Number: 2015960436

Mathematics Subject Classification (2010): 65Cxx, 65C99, 68U20

Springer Cham Heidelberg New York Dordrecht London
© Springer International Publishing Switzerland 2016

This work is subject to copyright. All rights are reserved by the Publisher, whether the whole or part of the material is concerned, specifically the rights of translation, reprinting, reuse of illustrations, recitation, broadcasting, reproduction on microfilms or in any other physical way, and transmission or information storage and retrieval, electronic adaptation, computer software, or by similar or dissimilar methodology now known or hereafter developed.

The use of general descriptive names, registered names, trademarks, service marks, etc. in this publication does not imply, even in the absence of a specific statement, that such names are exempt from the relevant protective laws and regulations and therefore free for general use.

The publisher, the authors and the editors are safe to assume that the advice and information in this book are believed to be true and accurate at the date of publication. Neither the publisher nor the authors or the editors give a warranty, express or implied, with respect to the material contained herein or for any errors or omissions that may have been made.

Printed on acid-free paper

Springer International Publishing AG Switzerland is part of Springer Science+Business Media
(www.springer.com)

Contents

Part I Physics

Thermodynamics with 2 + 1 + 1 Dynamical Quark Flavors	5
Stefan Krieg for the Wuppertal-Budapest Collaboration	
Numerical Evaluation of Multi-Loop Feynman Integrals	15
Alexander Kurz, Peter Marquard, and Matthias Steinhauser	
MCTDHB Physics and Technologies: Excitations and Vorticity, Single-Shot Detection, Measurement of Fragmentation, and Optimal Control in Correlated Ultra-Cold Bosonic Many-Body Systems	23
Ofir E. Alon, Vanderlei S. Bagnato, Raphael Beinke, Ioannis Brouzos, Tommaso Calarco, Tommaso Caneva, Lorenz S. Cederbaum, Mark A. Kasevich, Shachar Klaiman, Axel U.J. Lode, Simone Montangero, Antonio Negretti, Ressa S. Said, Kaspar Sakmann, Oksana I. Streltsova, Marcus Theisen, Marios C. Tsatsos, Storm E. Weiner, Tomos Wells, and Alexej I. Streltsov	
PAMOP Project: Petaflop Computations in Support of Experiments	51
B.M. McLaughlin, C.P. Ballance, M.S. Pindzola, S. Schippers, and A. Müller	
Monte Carlo Simulation of Crystal-Liquid Phase Coexistence	75
Antonia Statt, Fabian Schmitz, Peter Virnau, and Kurt Binder	
A New Colloid Model for Dissipative-Particle-Dynamics Simulations	89
Jiajia Zhou and Friederike Schmid	
Force Field Optimization for Ionic Liquids: FFOIL	101
Konrad Breitsprecher, Narayanan Krishnamoorthy Anand, Jens Smiatek, and Christian Holm	

The Small Scale Structure of the Universe	119
Stefan Gottlöber, Chris Brook, Ilian T. Iliev, and Keri L. Dixon	
Part II Molecules, Interfaces, and Solids	
Ab Initio Transport Calculations for Functionalized Graphene Flakes on a Supercomputer	139
Michael Walz, Alexei Bagrets, Ferdinand Evers, and Ivan Kondov	
Solving the Scattering Problem for the P3HT On-Chain Charge Transport	155
A. Lücke, U. Gerstmann, S. Sanna, M. Landmann, A. Riefer, M. Rohrmüller, N.J. Vollmers, M. Witte, E. Rauls, R. Hölscher, C. Braun, S. Neufeld, K. Holtgrewe, and W.G. Schmidt	
Ab-Initio Calculations of the Vibrational Properties and Dynamical Processes in Semiconductor Nanostructures	171
Gabriel Bester and Peng Han	
Large-Scale Modeling of Defects in Advanced Oxides: Oxygen Vacancies in BaZrO₃ Crystals	187
Marco Arrigoni, Eugene A. Kotomin, and Joachim Maier	
Interfacial Properties and Growth Dynamics of Semiconductor Interfaces	199
Phil Rosenow, Andreas Stegmüller, Lisa Pecher, and Ralf Tonner	
Atomistic Simulation of Oligoelectrolyte Multilayers Growth	215
Pedro A. Sánchez, Jens Smiatek, Baofu Qiao, Marcello Sega, and Christian Holm	
Mechanochemistry of Cyclopropane Ring-Opening Reactions	229
Miriam Wollenhaupt, Martin Zoloff, and Dominik Marx	
Part III Bioinformatics	
Computational Modeling of a Biocatalyst at a Hydrophobic Substrate Interface	241
Sven Benson and Jürgen Pleiss	
Dynathor: Dynamics of the Complex of Cytochrome P450 and Cytochrome P450 Reductase in a Phospholipid Bilayer	255
Xiaofeng Yu, Daria B. Kokh, Prajwal Nandekar, Ghulam Mustafa, Stefan Richter, and Rebecca C. Wade	

Part IV Reactive Flows

Numerical Simulation of Turbulent Combustion with a Multi-Regional Approach 267

Feichi Zhang, Thorsten Zirwes, Peter Habisreuther, and Henning Bockhorn

Numerical Simulations of Rocket Combustion Chambers on Massively Parallel Systems 281

Roman Keller, Martin Seidl, Markus Lempke, Peter Gerlinger, and Manfred Aigner

Part V Computational Fluid Dynamics

High-Resolution Numerical Analysis of Turbulent Flow in Straight Ducts with Rectangular Cross-Section 301

Yoshiyuki Sakai and Markus Uhlmann

Investigation of Convective Heat Transfer to Supercritical Carbon Dioxide with Direct Numerical Simulation 315

Xu Chu and Eckart Laurien

DNS Investigation of the Primary Breakup in a Conical Swirled Jet 333

Claudio Galbiati, Moritz Ertl, Simona Tonini, G. Elvio Cossali, and Bernhard Weigand

Numerical Simulation of Subsonic and Supersonic Impinging Jets 349

Robert Wilke and Jörn Sesterhenn

On the Impact of Forward-Facing Steps on Disturbance Amplification in Boundary-Layer Flows 371

Christopher Edelmann and Ulrich Rist

Large-Scale Simulations of a Non-generic Helicopter Engine Nozzle and a Ducted Axial Fan 389

Mehmet Onur Cetin, Alexej Pogorelov, Andreas Lintermann, Hsun-Jen Cheng, Matthias Meinke, and Wolfgang Schröder

Large-Eddy Simulation of a Scramjet Strut Injector with Pilot Injection 407

Sebastian Eberhardt and Stefan Hickel

Turbulence Resolving Flow Simulations of a Francis Turbine with a Commercial CFD Code 421

Timo Krappel, Albert Ruprecht, and Stefan Riedelbauch

Numerical Investigation of a Full Load Operation Point for a Low Head Propeller Turbine 435

Bernd Junginger and Stefan Riedelbauch

Detached Eddy Simulation of Flow and Heat Transfer in Swirl Tubes	449
Christoph Biegger and Bernhard Weigand	
Evaluation and Control of Loads on Wind Turbines under Different Operating Conditions by Means of CFD	463
Christoph Schulz, Annette Fischer, Pascal Weihing, Thorsten Lutz, and Ewald Krämer	
Advances in Parallelization and High-Fidelity Simulation of Helicopter Phenomena	479
Patrick P. Kranzinger, Ulrich Kowarsch, Matthias Schuff, Manuel Keßler, and Ewald Krämer	
Numerical Study of Three-Dimensional Shock Control Bump Flank Effects on Buffet Behavior	495
R. Mayer, D. Zimmermann, K. Wawrzinek, T. Lutz, and E. Krämer	
High Fidelity Scale-Resolving Computational Fluid Dynamics Using the High Order Discontinuous Galerkin Spectral Element Method	511
Muhammed Atak, Andrea Beck, Thomas Bolemann, David Flad, Hannes Frank, and Claus-Dieter Munz	
Toward a Discontinuous Galerkin Fluid Dynamics Framework for Industrial Applications	531
Sebastian Boblest, Fabian Hempert, Malte Hoffmann, Philipp Offenhäuser, Matthias Sonntag, Filip Sadlo, Colin W. Glass, Claus-Dieter Munz, Thomas Ertl, and Uwe Iben	
A High-Order Discontinuous Galerkin CFD Solver for Turbulent Flows	547
Michael Wurst, Manuel Keßler, and Ewald Krämer	
Mesoscale Simulations of Anisotropic Particles at Fluid-Fluid Interfaces	565
Qingguang Xie, Florian Günther, and Jens Harting	
Highly Efficient Integrated Simulation of Electro-Membrane Processes for Desalination of Sea Water	579
Kannan Masilamani, Harald Klimach, and Sabine Roller	
Part VI Transport and Climate	
Application of the Regional Climate Model CCLM for Studies on Urban Climate Change in Stuttgart and Decadal Climate Prediction in Europe and Africa	593
H.-J. Panitz, G. Schädler, M. Breil, S. Mieruch, H. Feldmann, K. Sedlmeier, N. Laube, and M. Uhlig	

High-Resolution WRF Model Simulations of Critical Land Surface-Atmosphere Interactions Within Arid and Temperate Climates (WRFCLIM)..... 607
 Josipa Milovac, Oliver-Lloyd Branch, Hans-Stefan Bauer, Thomas Schwitalla, Kirsten Warrach-Sagi, and Volker Wulfmeyer

Do We Have to Update the Land-Use/Land-Cover Data in RCM Simulations? A Case Study for the Vu Gia-Thu Bon River Basin of Central Vietnam 623
 Ngoc Bich Phuong Nguyen, Patrick Laux, Johannes Cullmann, and Harald Kunstmann

Part VII Miscellaneous Topics

On Estimation of a Viral Protein Diffusion Constant on the Curved Intracellular ER Surface..... 641
 M.M. Knodel, A. Nägel, S. Reiter, M. Rupp, A. Vogel, M. Lampe, P. Targett-Adams, E. Herrmann, and G. Wittum

Application of Large-Scale Phase-Field Simulations in the Context of High-Performance Computing 659
 Johannes Hötzer, Marcus Jainta, Marouen Ben Said, Philipp Steinmetz, Marco Berghoff, and Britta Nestler

Large Scale Numerical Simulations of Planetary Interiors 675
 Ana-Catalina Plesa, Christian Hüttig, Maxime Maurice, Nicola Tosi, and Doris Breuer

Coupled PIC-DSMC Simulations of a Laser-Driven Plasma Expansion 689
 S. Copplesstone, T. Binder, A. Mirza, P. Nizenkov, P. Ortwein, M. Pfeiffer, S. Fasoulas, and C.-D. Munz

Part I Physics

Peter Nielaba

In this section, eight physics projects are described, which achieved important scientific results by using the HPC resources Hermit and Hornet of the HLRS. Fascinating new results are being presented in the following pages for quantum systems (elementary particle systems, ultra-cold bosonic systems, atomic and molecular collisions), soft matter systems (colloids, ionic liquids), and astrophysical systems (small scale structure of the universe).

In the last granting period, quantum mechanical properties of quarks and multi loop Feynman integrals have been investigated as well as atomic and molecular collisions and the quantum many body dynamics of trapped bosonic systems.

S. Krieg (University of Wuppertal) and the Wuppertal-Budapest collaboration in their project *HighPQCD* aim at a high precision calculation of the charmed equation of state of Quantum Chromodynamics (QCD). The principal investigators (PIs) use importance sampling methods for staggered fermions in a lattice discretized version of QCD. Following the PIs previous important investigations on the $N_f = 2+1$ flavor QCD equation of states, in the last granting period new results have been computed on the thermodynamics in the situation with a dynamical charm quark ($N_f = 2+1+1$) for $N_t = 12$, and on the neutron-proton and other mass splittings, using combined theories of quantum electrodynamics (QED) and QCD.

In the project (*NumFeyn*), A. Kurz, M. Steinhauser (both from KIT) and P. Marquard (DESY) evaluate multi-loop Feynman integrals in perturbative calculations in quantum field theories. By using Monte Carlo integration implemented in the FIESTA package (*Feynman Integral Evaluation by a Sector decomposiTiion*), in the last granting period the PIs have investigated the relation between two renormalization schemes (modified minimal subtraction and the on-shell scheme) for heavy quark masses, and quantum corrections to the anomalous magnetic moment of the muon, both at four-loop accuracy.

P. Nielaba (✉)

Fachbereich Physik, Universität Konstanz, 78457 Konstanz, Germany

e-mail: peter.nielaba@unikonstanz.de

O.E. Alon, V. S. Bagnato, R. Beinke, I. Brouzos, T. Calarco, T. Caneva, L.S. Cederbaum, M.A. Kasevich, S. Klaimann, A. U. J. Lode, S. Montangero, A. Negretti, R. S. Said, K. Sakmann, O. I. Streltsova, M. Theisen, M. C. Tsatsos, S. E. Weiner, T. Wells, A. I. Streltsov from the Universities and research centers of Haifa (OEA), Sao Paulo (VSB, MCT), Heidelberg (RB, LSC, SK, MT, AIS), Ulm (IB, TC, SM, RSS), Barcelona (TC), Stanford (MAK, KS), Basel (AUJL), Hamburg (AN), Dubna (OIS), Berkeley (SEW), and Cambridge (TW) studied in their project *MCTDHB* properties of interacting ultra-cold bosonic many-body systems by their method termed *Multi-Configurational Time-Dependent Hartree method for Bosons*. MCTDHB targets at many-body effects beyond the mean-field level, in particular at a loss of coherence and fragmentation. The PIs continued their exploration of the physics of trapped interacting ultra-cold systems at the full many-body level by solving the underlying time- (in)dependent many-boson Schrödinger equation within the framework of the MCTDHB method.

In the last granting period, the PIs investigated the static properties and the many-body dynamics of vortices in two-dimensional (2D) and three-dimensional (3D) quantum objects carrying angular momentum, confined in parabolic traps and circular traps with double-well-like topologies, with particular emphasis on the loss of the coherence and the build-up of the fragmentation. In 2D harmonic traps, new many-body modes of quantized vorticity (*phantom vortices*) have been found, and connections between the resonant reaction of a Bose-Einstein condensate (BEC) stirred by a rotating laser beam and fragmentation. The properties of 2D BECs in circular traps have been explored as well, in particular the effect of time-dependent barriers on the stability against ground-state fragmentation. In the anisotropically-confined 3D systems the PIs discovered a new mechanism of vortex reconnections.

The PIs developed the MCRDHB method further, in particular the linear-response on-top of the MCTDHB method (LR-MCTDHB), providing access to the many-body excited states. By this method, the PIs classified the excited states into a mean-field-like group and a many-body-like group. In the project, MCTDHB as well has been combined with the optimal-control algorithm CRAB, in order to manipulate and control interacting quantum many-body systems, and the combined method CRAB-MCTDHB has been applied to the investigation of quantum speed limit in a bosonic Josephson junction setup. The MCTDHB package, its LR-MCTDHB extension, as well as collections of the tools for the analysis, visualization, package-making, building, teaching, and development, have been integrated in MCTDHB-Lab, a java-based environment.

In addition, the PIs propose a new analysis tool capable of simulating the outcomes of typical shots generated in the experimental detection of ultra-cold atomic systems and describe an experimental protocol capable of a direct quantitative measurement of the fragmentation in trapped bosonic systems.

B. M. McLaughlin, C. P. Ballance, M. S. Pindzola, S. Schippers and A. Müller from the Universities of Belfast (BMM), Auburn (CPB and MSP) and Giessen (SS and AM) investigated in their project *PAMOP* atomic, molecular and optical collisions on petaflop machines. The Schrödinger and Dirac equations have been solved with the R-matrix or R-matrix with pseudo-states approach, and the time

dependent lattice (TDL) method has been used for charge exchange problems. Various experimentally relevant systems and phenomena have been investigated, ranging from photoionization cross sections, resonance energy positions, to Auger widths and strengths in valence- (Ca^+ , W , W^+) or inner-shell- (O^+ , O^{2+} , O^{3+}) systems, and charge transfer cross sections in C^{6+} collisions with H and He atoms.

The studies of the (colloidal) soft matter systems have focused on the crystal-liquid phase coexistence and their dynamical properties, and on the properties of ionic liquids in confinement.

A. Statt, F. Schmitz, P. Virnau and K. Binder from the University of Mainz in their project *colloid* developed a general method to study crystal nuclei and to obtain estimates for the free energy barrier against homogeneous nucleation. In their Monte Carlo studies, the PIs used a “softened” version of the effective Asakura-Oosawa model, with an effective potential between the colloids which is everywhere continuous, they computed the solid-liquid interface excess free energy via the ensemble switch method, and they obtained the pressure at phase coexistence from the interface velocity method. The PIs showed that the surface excess free energy can be determined accurately from Monte Carlo simulations over a wide range of nucleus volumes, and they found that the resulting nucleation barriers are independent of the size of the total system volume. In addition, the PIs results show that the nucleus shape is almost spherical, when the anisotropy of the interface tension is in the order of a few per cent, and the results were discussed in the frame of the classical nucleation theory.

J. Zhou and F. Schmid from the University of Mainz in their project *CCAC* have developed a mesoscopic colloid model based on the dissipative particle dynamics. In this model, the colloid is represented by a large spherical bead, and its surface interacts with solvent beads through a pair of dissipative and random forces, extending the tunable-slip boundary method from planar surfaces, as introduced by one of the PIs (FS) in previous works, to curved geometry. The PIs computed the diffusion constant of a single colloid in a cubic box, using the program package ESPRESSO, and found good agreement with the predictions from hydrodynamic theories.

K. Breitsprecher, N.K. Anand, J. Smiatek and C. Holm from the University of Stuttgart in their project *FFOIL* explored different models of room temperature ionic liquids (RTILs) in confined environment and bulk solution by molecular dynamics (MD) simulations with the software packages ESPRESSO and Gromacs as well as other MD-codes. In the last granting period, the PIs focused on algorithms for metal boundary conditions in various geometries, and on effects of graphite structure on the adsorbed ions in planar capacitor geometries, in particular by comparing an explicit graphene structure to an unstructured planar Lennard-Jones surface and by investigating mixtures of the ionic liquid EMIM BF₄ with different concentrations of Acetonitril (ACN) in contact with carbide-derived carbon (CDC) electrodes. The PIs showed that the increased adsorption of the ionic liquid on graphite surfaces is due to the texturing influence of the honeycomb pattern.

On different length scales compared to the quantum and soft matter systems described above, the project *SSSU* has focused on the small scale structure of the

universe. In this project, S. Gottlöber, C. Brook, I.T. Iliev and K.L. Dixon from the Leibniz Institute for Astrophysics at Potsdam (SG) and the Universities of Madrid (CB) and Sussex (ITI, KLD) investigated reionization and galaxy formation processes. In their project, the PIs studied the role of reionization in the early stage of cosmological evolution, on the formation and evolution of the small scale structure, by three simulations, using the CubeP³M N-body code, the background cosmology based on WMAP 5-year data, the linear power spectrum of density fluctuations calculated with the code CAMB, initial conditions by the Zeldovich approximation for red shifts of 150, and radiative transfer simulations with their code C²-Ray. In addition, the PIs use the physical model of the MaGICC project (*Making Galaxies in a Cosmological Context*) and initial conditions of the CLUES project (*Constrained Local Universe Simulations*) to construct a model of the Local Group of galaxies, including the Milky Way, Andromeda, M33 and dwarf galaxies. As galaxy properties, rotation curves have been computed as well as stellar-to-halo mass relations and the mass of galaxy baryons as a function of their circular velocity (Baryonic Tully-Fisher relation).

Thermodynamics with $2 + 1 + 1$ Dynamical Quark Flavors

Stefan Krieg for the Wuppertal-Budapest Collaboration

Abstract We report on our calculation of the equation of state of Quantum Chromodynamics (QCD) from first principles, through simulations of Lattice QCD. We use an improved lattice action and $N_f = 2 + 1 + 1$ dynamical quark flavors and physical quark mass parameters. Now, we are in a position to present first results at $N_t = 12$.

1 Introduction

The aim of our project is to compute the charmed equation of state for Quantum Chromodynamics (for details, see [1]). We are using the lattice discretized version of Quantum Chromodynamics, called lattice QCD, which allows simulations of the theory through importance sampling methods. Our results are important input quantities for phenomenological calculations and are required to understand experiments aiming to generate a new state of matter, called Quark-Gluon-Plasma, such as the upcoming FAIR at GSI, Darmstadt.

Our simulations are performed using so-called staggered fermions. In the continuum limit, i.e. at vanishing lattice spacing a , one staggered Dirac operator implements four flavors of mass degenerate fermions. At finite lattice spacing, however, discretization effects induce an interaction between these would be flavors lifting the degeneracy. The “flavors” are, consequentially, renamed to “tastes”, and the interactions are referred to as “taste-breaking” effects. Even though the tastes are not degenerate, in simulations one takes the fourth root of the staggered fermion determinant to implement a single flavor. This procedure is not proven to be correct—however, practical evidence suggests that it does not induce errors visible with present day statistics.

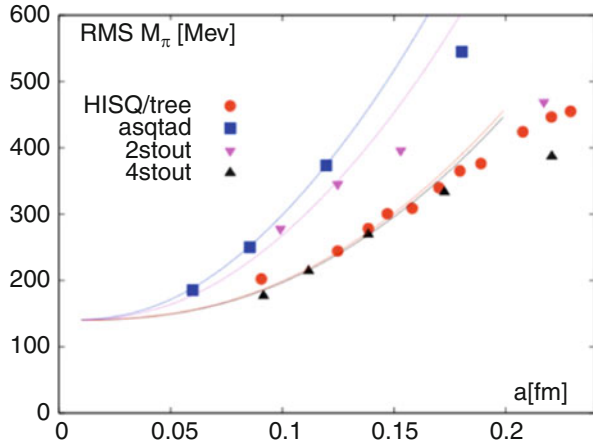
S. Krieg (✉)

Fachbereich C - Physik, Bergische Universität Wuppertal, 42119 Wuppertal, Germany

IAS, Jülich Supercomputing Centre, Forschungszentrum Jülich GmbH, 52425 Jülich, Germany

e-mail: krieg@uni-wuppertal.de

Fig. 1 RMS pion mass for different staggered fermion actions, in the continuum limit



Taste-breaking is most severely felt at low pion masses and large lattice spacing, as the pion sector is distorted through the taste-breaking artifacts: there is one would-be Goldstone boson, and 15 additional heavier “pions”, which results in an RMS pion mass larger than the mass of the would-be Goldstone boson. This effect is depicted in Fig. 1 for different staggered type fermion actions. As can be seen for this figure, the previously used twice stout smeared action (“2stout”) has a larger RMS pion mass and thus taste-breaking effects than the HISQ/tree action. If, however, the number of smearing steps is increased to four, with slightly smaller smearing strength (“4stout”), the RMS pion mass measured agrees with that of the HISQ/tree action. In order to have an improved pion sector, we, therefore, opted to switch to this new action and to restart our production runs.

So far, the equation of state is known only in 2+1 flavor QCD. Here, the status of the field is marked by our papers on the $N_f = 2 + 1$ equation of state [2, 3] (see Fig. 2). The contribution from the sea charm quarks most likely matter at least for $T > 300\text{--}400\text{ MeV}$ (for an illustration, see Fig. 3).

1.1 Reference Point: The $N_f = 2 + 1$ Equation of State

In [3] we have presented the first full calculation of the $N_f = 2 + 1$ Equation of State (EoS) of Quantum Chromodynamics (QCD) (still using our 2stout action). This result is the reference point for our calculation of the charmed EoS, and already included one continuum extrapolated result at $T = 214\text{ MeV}$ for the trace anomaly using our new lattice action including a dynamical charm quark ($N_f = 2 + 1 + 1$).

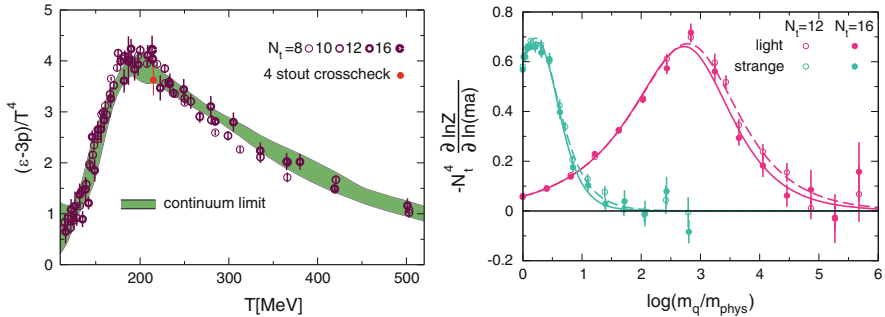


Fig. 2 *Left:* The trace anomaly as a function of the temperature. The continuum extrapolated result with total errors is given by the *shaded band*. Also shown is a cross-check point computed in the continuum limit with our new and different lattice action at $T = 214$ MeV, indicated by a *smaller filled red point*, which serves as a crosscheck on the peak's height. *Right:* Setting the overall scale of the pressure: integration from the infinitely large mass region down to the physical point using a range of dedicated ensembles and time extents up to $N_t = 16$; the sum of the areas under the curves gives p/T^4 . This result could be used for the cEoS normalization as well (see text)

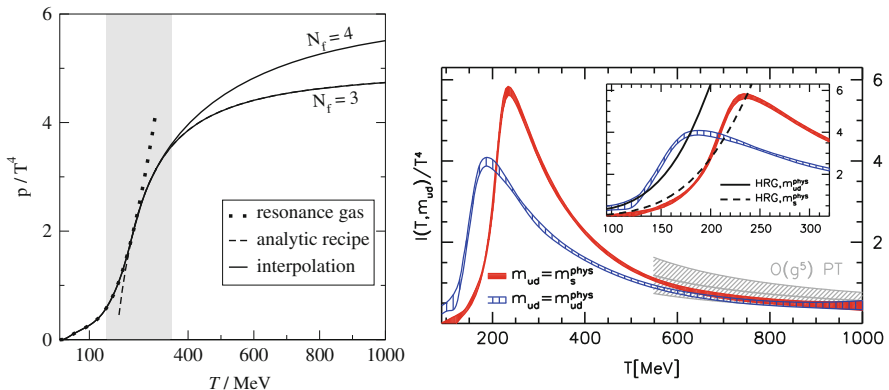


Fig. 3 *Left:* Laine and Schroeder's perturbative estimate of the effect of the charm in the QCD equation of state [4]. *Right:* Wuppertal-Budapest [2] and perturbative (up to $O(g^5)$) results for the equation of state

As visible in Fig. 2, at this temperature the charm quark is not yet relevant, since the $N_f = 2 + 1 + 1$ (continuum) data point falls right onto the (continuum) $N_f = 2 + 1$ curve. Below this temperature, we can compare the results with and without dynamical charm and can even use the $N_f = 2 + 1$ results to renormalize the $N_f = 2 + 1 + 1$ curve [5, 6].

2 Progress for the Charmed Equation of State

The $N_f = 2 + 1$ lattice results mentioned in the previous section agree with the HRG at low temperatures and are correct for the small to medium temperatures, and, as is shown in Fig. 3, at temperatures of about 1 GeV perturbative results become sufficiently precise. Therefore, we need to calculate the EoS with a dynamical charm only for the remaining temperatures in the region of approximately $300 \text{ MeV} < T < 1000 \text{ MeV}$.

We are using our 4stout lattice action for these calculations. The crosscheck point shown in Fig. 2 was computed using this new action. Since it perfectly agrees with the $N_f = 2 + 1$ results, even though it was computed using a dynamical charm, we can be certain that at temperatures at and below $T = 214 \text{ MeV}$, we can rely on the $N_f = 2 + 1$ results.

Our preliminary results are shown in Fig. 4, all errors are statistical only. Our results span a region of temperatures from $T = 214 \text{ MeV}$ up to $T = 1.2 \text{ GeV}$. At the low end we make contact to the $N_f = 2 + 1$ equation of state, and at large temperatures to the HTL result. Thereby, we cover the full region of temperatures, from low temperatures, where the HRG gives reliable results, to high temperatures, where we make contact with perturbation theory. The figure contains **new data points** at $N_f = 12$ generated in the last period.

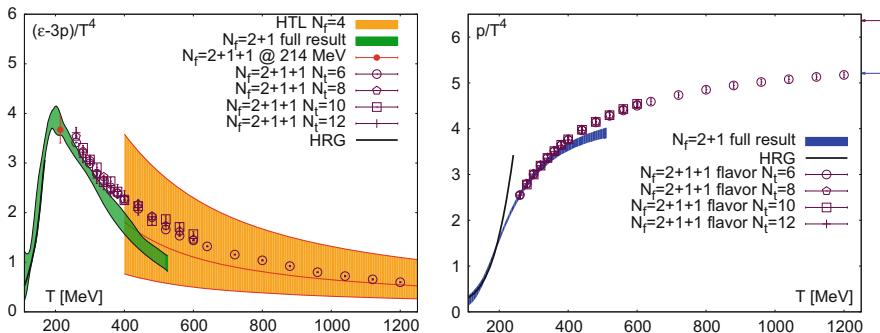


Fig. 4 *Left*: Preliminary results for the charmed EoS. For comparison, we show the HRG result, the $N_f = 2 + 1$ band, and, at high Temperatures, the HTL result [7], where the *central line* marks the HTL expectation for the EoS with the band resulting from (large) variations of the renormalization scale. *Right*: Preliminary result for the pressure, errors indicate the Stefan-Boltzmann value. All errors are statistical only

2.1 Line of Constant Physics

With the switch to a new lattice action comes the need to (re-) compute the LCP. In order to be able to reach large temperatures ($\beta > 4$), we have extended these calculations since the last report. Since we would like to span the temperature range from approximately $300 \text{ MeV} < T < 1000 \text{ MeV}$, we have to compute the LCP for a large range of couplings or lattice spacings. We split this range up in three overlapping regions (since we have to make sure that the derivative is smooth) according to the applicable simulation strategies.

At medium to coarse lattice spacings (region I) one can afford to use spectroscopy to tune the parameters. This is shown in Fig. 5. Here, we bracketed the physical point defined through M_π/f_π and $(2M_K - M_\pi)/f_\pi$ and, through interpolation, tune the light and strange quark masses to per-mill precision.

Using the parameters computed in this way, we then performed simulations on JUROPA at the SU(3) flavor-symmetrical point [8], extrapolating the results to our target couplings. There, we tuned the parameters to reproduce the extrapolated results. Since the quark masses are larger than physical, such simulations are considerably less costly than using spectroscopy as for region I, and we are thus able to compute a precise LCP down to fine lattice spacings of $a = 0.05 \text{ fm}$ (region II), where the HMC starts being affected by the freezing of topology (Fig. 6).

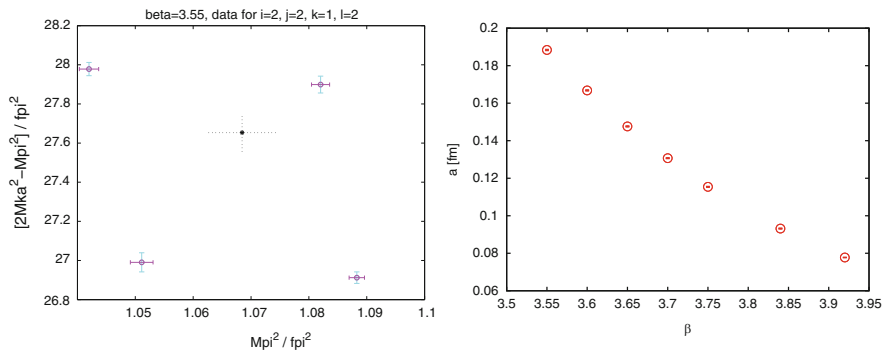


Fig. 5 Region of the LCP, for coarse to medium lattice spacing ($a > 0.08 \text{ fm}$). Here, dedicated simulations bracketing the physical point archive a sub-percent accuracy for the LCP. *Left*: Bracketing of the physical point defined through M_π/f_π and $(2M_K - M_\pi)/f_\pi$. The strange quark mass is tuned (m_s/m_l is not fixed) and the ratio of the charm to strange quark mass is set at $m_c/m_s = 11.85$. *Right*: LCP computed through spectroscopy

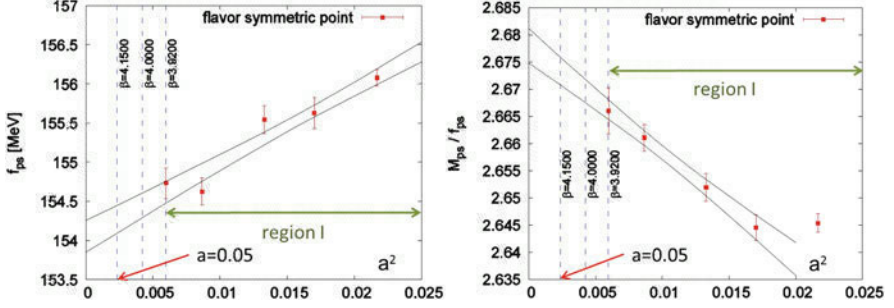


Fig. 6 Using the LCP computed from spectroscopy for coarse to medium lattice spacings (region I), dedicated simulations in the SU(3) flavor-symmetrical point [8] using these parameters are extrapolated towards the continuum. At the target coupling, the parameters are tuned until they reproduce the extrapolated value. In this way the LCP is extended to medium to small lattice spacings of $0.08 > a > 0.05$ fm (region II)

For finer lattice spacings we thus used our established step scaling procedure [3] based on the w_0 scale. To this end, we computed the observable

$$\mathcal{O} = t \frac{d}{dt} [t^2 E(t)] \Big|_{0.01L^2}$$

at three different lattice spacings (a_0, a_1, a_2) and volumes ($16^4, 20^4, 24^4$) chosen to keep the physical volume fixed, extrapolated to $a_3 = 24/32a_2$, and tuned the coupling to match the extrapolated result. Using this method, we extended the LCP to very fine lattice spacings with $a < 0.05$ fm (region III).

2.2 Additional Results

In another effort, we calculated the neutron-proton and other mass splittings from first principles [9], using simulations of the combined theories of Quantum Electro- and Quantum Chromodynamics. Here, we used Hermit for valence calculations, i.e. we analyzed configurations generated elsewhere, computing the mass difference for a number of different bare parameters. The complete result is shown in Fig. 7. Due to the long range nature of Quantum Electrodynamics (QED) these simulations face significant finite-size effects, inducing shifts in the results considerably larger than the signal. Through analytical calculations (see SOM of [9]), we were able to predict and thus subtract these effects. Another important step was the development of a new update algorithm for the QED, which reduced the autocorrelation by more than 2 orders of magnitude.

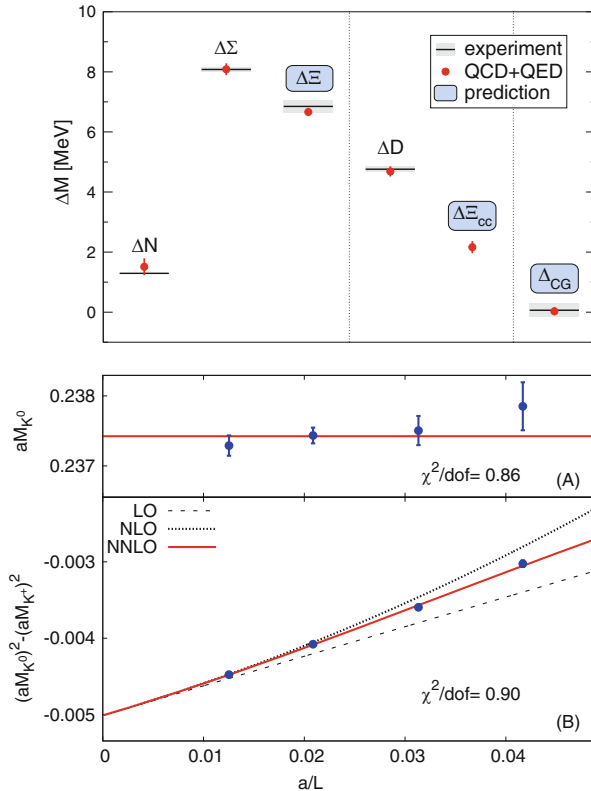


Fig. 7 *Left*: Mass splittings. The *horizontal lines* are the experimental values and the *grey shaded regions* represent the experimental error. Our results are shown by *red dots* with their uncertainties. Splittings which have either not been measured in experiment or are measured with less precision than in our calculation are indicated by a *blue shaded region* around the label. *Right*: Finite-volume behavior of kaon masses. (A) The neutral kaon mass, M_{K^0} , shows no significant finite volume dependence; L denotes the linear size of the system. (B) The mass-squared difference of the charged kaon mass, M_{K^+} , and M_{K^0} indicates that M_{K^+} is strongly dependent on volume. This finite-volume dependence is well described by an analytical results [9] (Figures taken from *Science* **347** 1452, reference [9]. Reprinted with permission from AAAS.)

3 Production Specifics and Performance

Most of our production is done using modest partition sizes, as we found these to be most efficient for our implementation.

3.1 Performance

Our code shows nice scaling properties on HERMIT and HORNET. For our scaling analysis below, we used two lattices ($N_s = 32$ and 48) and several partition sizes up to 256 nodes (HERMIT). We timed the most time consuming part of the code: the fermion matrix multiplication. The results are summarized in the following table:

No. of nodes	Gflop/node $N_s = 32$	Gflop/node $N_s = 48$
1	16.3	15.4
2	16.8	16.0
4	16.5	16.2
8	16.3	16.3
16	16.3	16.3
32	16.8	16.0
64	17.1	16.5
128	19.2	16.5
256	16.3	16.0

Test show that our scaling on HORNET is similarly good - however at a higher performance of ≈ 22 and ≈ 21 Gflop/s for the $N_s = 32$ and $N_s = 48$ lattices, respectively.

3.2 Production

Given the nice scaling properties of our code, we were able to run at the sweet spot for queue throughput, which we found to be located at a job size of 64 nodes. Larger job sizes proved to have a scheduling probability sufficiently low that benefits in the runtime due to the larger number of cores were compensated and the overall production throughput decreased. We, therefore, opted to stay at jobs sizes with 64 nodes.

4 Outlook

We believe we will be able to publish within the year. HERMIT and HORNET have proved to be essential tools enabling us to achieve this goal.

5 Publications of the Project

5.1 Peer-Reviewed

- [9] *Ab initio calculation of the neutron-proton mass difference*, *Science* **347** (2015) 1452–1455
- [10] *Equation of state, fluctuations and other recent results from LQCD*, Proceedings of the 30th Winter Workshop on Nuclear Dynamics (WWND 2014), *J.Phys.Conf.Ser.* **535** (2014) 012016

5.2 Other

- [11] *From quarks to hadrons and back - spectral and bulk phenomena of strongly interacting matter*, Proceedings of the XXVI IUPAP Conference on Computational Physics (CCP2014), *J. Phys. Conf. Ser.* **640** (2015) 012053
- [12] *Recent results on the Equation of State of QCD*, Proceedings of the 32nd International Symposium on Lattice Field Theory (Lattice 2014), *PoS(LATTICE2014)* 224

References

1. Borsanyi, S., Endrodi, G., Fodor, Z., Katz, S.D., Krieg, S., et al.: The QCD equation of state and the effects of the charm. *PoS LATTICE2011*, 201 (2011). [[1204.0995](#)]
2. Borsanyi, S., Endrodi, G., Fodor, Z., Jakovac, A., Katz, S.D., et al.: The QCD equation of state with dynamical quarks. *J. High Energy Phys.* **1011**, 077 (2010). [[1007.2580](#)]
3. Borsanyi, S., Fodor, Z., Hoelbling, C., Katz, S.D., Krieg, S., et al.: Full result for the QCD equation of state with 2+1 flavors *Phys. Lett.* **B730**, 99–104 (2014). [[1309.5258](#)]
4. Laine, M., Schroder, Y.: Quark mass thresholds in QCD thermodynamics. *Phys. Rev.* **D73** 085009 (2006). [[hep-ph/0603048](#)]
5. Endrodi, G., Fodor, Z., Katz, S., Szabo, K.: The equation of state at high temperatures from lattice QCD. *PoS LAT2007*, 228 (2007). [[0710.4197](#)]
6. Borsanyi, S., Endrodi, G., Fodor, Z., Katz, S., Szabo, K.: Precision SU(3) lattice thermodynamics for a large temperature range. *J. High Energy Phys.* **1207**, 056 (2012). [[1204.6184](#)]
7. Andersen, J.O., Leganger, L.E., Strickland, M., Su, N.: Three-loop HTL QCD thermodynamics. *J. High Energy Phys.* **1108**, 053 (2011). [[1103.2528](#)]
8. Bietenholz, W., Bornyakov, V., Gockeler, M., Horsley, R., Lockhart, W., et al.: Flavour blindness and patterns of flavour symmetry breaking in lattice simulations of up, down and strange quarks. *Phys. Rev.* **D84**, 054509 (2011). [[1102.5300](#)]
9. Borsanyi, S., Durr, S., Fodor, Z., Hoelbling, C., Katz, S., et al.: Ab initio calculation of the neutron-proton mass difference. *Science* **347**, 1452–1455 (2015). [[1406.4088](#)]

10. Wuppertal-Budapest Collaboration, Krieg, S.: Equation of state, fluctuations and other recent results from LQCD. In: Proceedings of the 30th Winter Workshop on Nuclear Dynamics (WWND 2014) (2014); J. Phys. Conf. Ser. **535**, 012016 (2014). doi:10.1088/1742-6596/535/1/012016
11. Budapest-Marseille-Wuppertal Collaboration, Wuppertal-Budapest Collaboration, Krieg, S.: From quarks to hadrons and back - spectral and bulk phenomena of strongly interacting matter. In: Proceedings of the 26th Conference on Computational Physics (CCP 2014) (2014); J. Phys. Conf. Ser. **640**(1), 012053 (2015). doi:10.1088/1742-6596/640/1/012053
12. Borsányi, S., Fodor, Z., Hoelbling, C., Katz, S.D., Krieg, S., Ratti, C., Szabo, K.K.: Recent results on the equation of state of QCD. In: Proceedings of the 32nd International Symposium on Lattice Field Theory (Lattice 2014) (2014); PoS **LATTICE2014**, 224 (2015) [arXiv:1410.7917]

Numerical Evaluation of Multi-Loop Feynman Integrals

Alexander Kurz, Peter Marquard, and Matthias Steinhauser

Abstract The aim of this project is the evaluation of multi-loop Feynman integrals occurring in perturbative calculations within quantum field theories. The integrals under consideration enter the relation between the $\overline{\text{MS}}$ and on-shell definition of heavy quark masses and the anomalous magnetic moment of the muon. Both quantities are considered at four-loop accuracy. This report covers the period from May 2014 to April 2015.

1 Introduction

The main aim of modern particle physics is the exploration of the fundamental interaction between the elementary particles. Insight to this question is obtained by confronting high-precision calculations performed within the underlying relativistic quantum field theory with experimental data. The most powerful method to evaluate quantum corrections is perturbation theory which requires the evaluation of multi-loop integrals of the form

$$\int d^d p_1 \cdots d^d p_L \prod_i \frac{1}{k_i^2 - m_i^2}, \quad (1)$$

A. Kurz

Deutsches Elektronen-Synchrotron DESY, Platanenallee 6, 15738 Zeuthen, Germany

Institut für Theoretische Teilchenphysik, Karlsruher Institut für Technologie, 76128 Karlsruhe, Germany

e-mail: alexander.kurz2@kit.edu

P. Marquard

Deutsches Elektronen-Synchrotron DESY, Platanenallee 6, 15738 Zeuthen, Germany

e-mail: peter.marquard@desy.de

M. Steinhauser (✉)

Institut für Theoretische Teilchenphysik, Karlsruher Institut für Technologie, 76128 Karlsruhe, Germany

e-mail: Matthias.Steinhauser@kit.edu

where p_i and k_i are 4-vectors. p_i are integration variables and k_i are linear combinations of p_i and possible external momenta. Note that the dimension d is given by $d = 4 - 2\epsilon$ where ϵ serves as regularization parameter which is sent to zero after the integrations are performed.

In this project a special class of integrals is considered, so-called on-shell integrals with one external momentum, q , which fulfills the relation $q^2 = m^2$. In particular we also have for the masses $m_i = m$ or $m_i = 0$. Integrals of this type have been studied in the literature up to three loops (see, e.g., [1]), a systematic study at four loops (i.e. $L = 4$) is, however, missing.

Our investigations are driven by the following physical problems which we would like to address. The first one is concerned with the definition of the heavy quark masses which appear as fundamental parameters in the underlying Lagrange density. More precisely, we want to compute the relation between the $\overline{\text{MS}}$ and on-shell definition with four-loop accuracy within Quantum Chromodynamics (QCD). For the second physical quantity we consider Quantum Electrodynamics (QED) as our fundamental theory and evaluate quantum corrections to the anomalous magnetic moment of the muon, which in the recent years has been measured with high accuracy.

Calculations within perturbation theory involve several steps which include the automatic generation of all contributing Feynman diagrams, the translation to mathematical expressions and the manipulation of the latter such that the physical quantity is expressed as a linear combination of several thousands, sometimes even millions of integrals. In a next step the so-called Laporta algorithm [2] is applied in order to reduce the number of integrals. In our case we end up with about 400 integrals, so-called master integrals, similar to the one in Eq. (1) for $L = 4$ which have to be computed. In this project we apply numerical methods to compute the master integrals at the HLRS on the Hermit and Hornet computer cluster.

2 Program Package and Technical Details

The workhorse for the calculations which we are performing at the HLRS is the program package FIESTA [3–5], which has been developed since 2008 with the participation of the Institute for Theoretical Particle Physics (TTP) at KIT. FIESTA stands for Feynman Integral Evaluation by a Sector decomposition and applies the method of sector decomposition [6] to obtain finite expression for the coefficients of the Laurent series of Eq. (1) in $\epsilon = (4 - d)/2$. These finite expressions are multi-dimensional parameter integrals with in general large integrands of the size of a few hundred MB up to a GB.

In practice the preparation of the integrand is performed within Mathematica on the local cluster. The expressions are transferred in form of a data base to the HLRS where the time-consuming Monte-Carlo integration is performed. FIESTA uses a simple master slave model for the parallelization, where the integrands are distributed from the master to the slaves using MPI and each term is integrated using a single core by the slave.

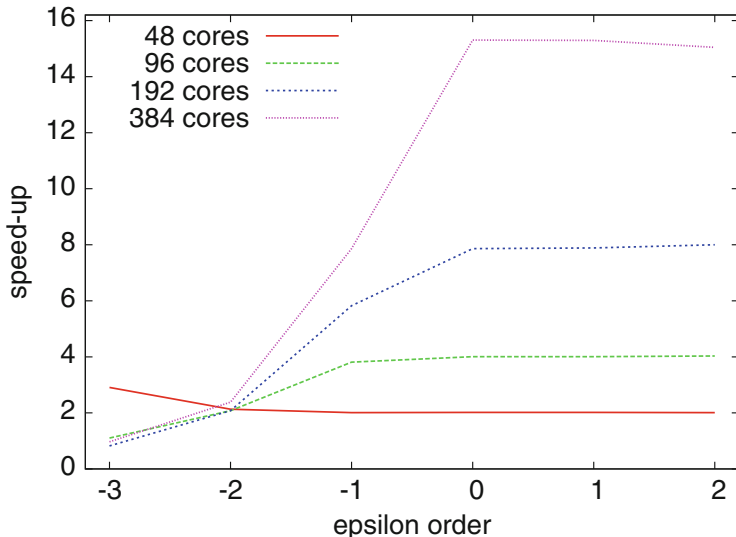


Fig. 1 Achieved speed-up for the sample integral shown in Fig. 2 needed for our calculation. The calculations have been performed on the `Hornet` cluster. The baseline is given by a run with 24 cores

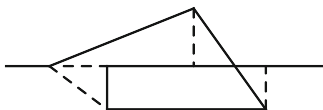


Fig. 2 Sample Feynman diagram appearing in the calculation of the $\overline{\text{MS}}$ -on-shell relation at four-loop order. *Solid and dashed lines* denote massive and massless lines, respectively

In Fig. 1 we show a typical speedup behaviour which we observe for the integrals on the `Hornet` cluster. On the x axis we show the ϵ order of the integral corresponding to the diagram in Fig. 2 and the y axis shows the speed-up as compared to the use of 24 cores. Note that the lower orders of the expansion in ϵ (i.e. order $1/\epsilon^k$ with $k = 1, 2$ and 3) contain only a few quite simple terms and thus there is no gain from using more cores. Furthermore, their contribution to the total CPU time for the considered diagram is only marginal. For the higher ϵ terms (ϵ^k with $k = 0, 1$ and 2), however, we find a near optimal speed-up behaviour.

For our calculation we used up to 1024 cores on `Hermit` and up to 576 cores on `Hornet`. For about 20 % of the integrals we used more than 256 cores. In this way we could respect the CPU time limit of 24 h and at the same time obtain the required precision.

All integrals were calculated multiple times with different precision to ensure the convergence of the Monte-Carlo integration. We observe the expected $1/\sqrt{N}$ behaviour in the reduction of the statistical uncertainty where N is the number of sample point.

3 Heavy Quark Mass Relations to Four Loops

In the Standard Model of particle physics the masses of the quarks are free parameters and in addition due to renormalization they are also scheme dependent. Two such renormalization schemes are the $\overline{\text{MS}}$ (modified minimal subtraction) and the on-shell scheme. Within perturbation theory one can obtain relations between these two schemes.

To obtain the $\overline{\text{MS}}$ -on-shell relation it is convenient to start with the relations between bare mass m_0 , which is present in the original Lagrange density, and $\overline{\text{MS}}$ mass m or on-shell mass M

$$m^0 = Z_m^{\overline{\text{MS}}} m, \quad m^0 = Z_m^{\text{OS}} M. \quad (2)$$

$Z_m^{\overline{\text{MS}}}$ and Z_m^{OS} denote the corresponding renormalization constants. $Z_m^{\overline{\text{MS}}}$ is known to four loops and can be found in [7–9]. By construction, the ratio of the two equations in (2) is finite which leads to

$$z_m(\mu) = \frac{m(\mu)}{M}, \quad (3)$$

where μ is the renormalization scale. z_m depends on $\alpha_s(\mu)$ and $\log(\mu/M)$ and has the following perturbative expansion

$$z_m(\mu) = \sum_{n \geq 0} \left(\frac{\alpha_s(\mu)}{\pi} \right)^n z_m^{(n)}(\mu), \quad (4)$$

with $z_m^{(0)} = 1$. The $\overline{\text{MS}}$ -on-shell relation has been calculated at one-, two-, and three-loop order in [10–15], respectively. Fermionic four-loop corrections with two massless insertions have been computed in [16].

To obtain the complete four-loop result for $z_m(\mu)$ one has to calculate Z_m^{OS} to this order. We followed standard techniques to perform the calculation and finally obtained $z_m(\mu)$ as a linear combination of 386 four-loop integrals. The simple integrals can be computed using (semi-)analytic methods. However, for 332 integrals FIESTA has been applied as described in the previous section. We insert the numerical results in our analytic expression and add the uncertainties in quadrature. The resulting uncertainty, which is interpreted as standard deviation, is multiplied by five to obtain a conservative error estimate.

Our final result for the four-loop coefficient in the expansion (4) specified to the three heavy quark of the Standard Model, charm (“ $n_l = 3$ ”), bottom (“ $n_l = 4$ ”) and top (“ $n_l = 5$ ”) reads [17]

$$\begin{aligned} z_m^{(4)} \Big|_{n_l=3} &= -1744.8 \pm 21.5 - 703.48 l_{\text{OS}} - 122.97 l_{\text{OS}}^2 \\ &\quad - 14.234 l_{\text{OS}}^3 - 0.75043 l_{\text{OS}}^4, \end{aligned}$$

$$\begin{aligned}
 z_m^{(4)} \Big|_{n_l=4} &= -1267.0 \pm 21.5 - 500.23 l_{OS} - 83.390 l_{OS}^2 \\
 &\quad - 9.9563 l_{OS}^3 - 0.514033 l_{OS}^4, \\
 z_m^{(4)} \Big|_{n_l=5} &= -859.96 \pm 21.5 - 328.94 l_{OS} - 50.856 l_{OS}^2 \\
 &\quad - 6.4922 l_{OS}^3 - 0.33203 l_{OS}^4,
 \end{aligned} \tag{5}$$

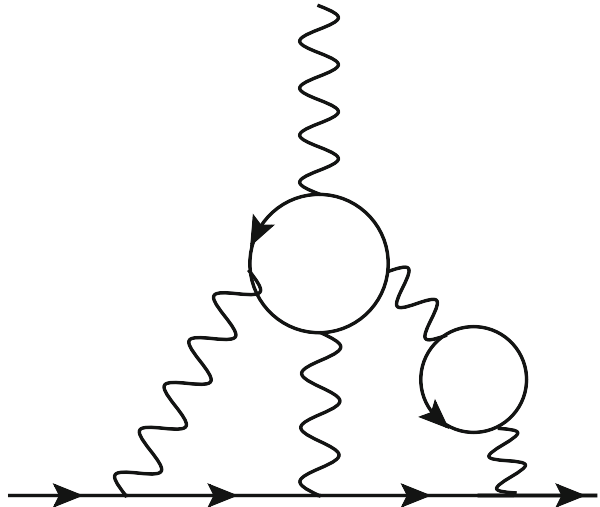
with $l_{OS} = \ln(\mu^2/M^2)$. We obtain coefficients with an accuracy of 1.2% for $n_l = 3$, 1.7% for $n_l = 4$ and 2.5% for $n_l = 5$, where the given errors stem solely from the numerical integration within FIESTA. The obtained precision is at the moment sufficient for phenomenological applications. The obtained results in Eq. (5) are crucial for the precise extraction of numerical values for the heavy quark masses. Phenomenological examples are discussed in [17].

4 Anomalous Magnetic Moment of the Muon

At the classical level the leptonic anomalous magnetic moment, $a = (g - 2)/2$, is predicted to be equal to zero. The deviation from zero is due to quantum corrections which have been investigated since the 1940s. Nowadays the experimental results have reached such a high precision [18, 19] that four- and even five-loop corrections [20, 21] are necessary to perform a sensible comparison.

An ongoing project of our working group is the evaluation of four-loop corrections involving closed electron loops to the anomalous magnetic moment of the muon. A sample Feynman diagram is shown in Fig. 3 for which we will present preliminary result in the following.

Fig. 3 Sample Feynman diagram contribution to $(g - 2)$ of the muon at four-loop order. *Solid and wiggled lines* denote leptons and photons, respectively. In this example the *closed fermion loops* correspond to electrons whereas the external leptons are muons



As compared to the $\overline{\text{MS}}$ -on-shell relation discussed in the previous section there is the additional complication that we have two mass scales, the electron and the muon masses, m_e and m_μ . Due to the strong hierarchy, $m_e \ll m_\mu$, it is suggestive to consider an expansion in m_e/m_μ . Prescriptions to perform such an expansion at the level of integrands can be found in [22] and have been implemented by our group. This allows us to obtain the anomalous magnetic moment as a linear combination of integrals which have already been considered in Sect. 3, where the dimensionful scale is given by the muon mass, and new type of integrals, which contain m_e as mass scale. Computing also the new type of master integrals on the `Hornet` cluster leads to the contribution of the diagrams in Fig. 3 to the muon anomalous magnetic moment

$$(115.19 \pm 0.03) + (1.60 \pm 0.04) + \dots, \quad (6)$$

where the numbers in the first and second bracket come from the $(m_e/m_\mu)^0$ and $(m_e/m_\mu)^1$ contributions, respectively; the ellipsis indicate higher order corrections in the mass ratio which are expected to be small. Our preliminary result agrees well with the result from [23].

5 Conclusions and Outlook

It has been shown that the package `FIESTA` performs well on the clusters `Hermit` and `Hornet`. A good speedup behaviour is observed up to 384 cores which allowed us to obtain sufficiently precise results of all relevant integrals within the CPU time limit of 24 h. The results have been used to obtain for the first time the relation between the $\overline{\text{MS}}$ and on-shell heavy quark mass which is published in [17].

In [17] the number of colours (present in QCD) is set to the physical value, i.e. $N_c = 3$. In a next step we want to obtain results for a generic value of N_c which requires an increase of the accuracy of the master integrals. On the one hand we will further improve `FIESTA`. On the other hand we will try to optimize the number of cores which shall be used for a given integral.

As far as the anomalous magnetic moment of the muon is concerned we have to further study the new kind of integrals which occur in the power-corrections proportional to m_e/m_μ . In particular, we have to optimize their representation for the numerical integration on `Hornet`.